

1 **Development and clinical evaluation of a monkeypox antigen-detecting rapid**  
2 **diagnostic test**

3 Nobuyuki Kurosawa<sup>1,2</sup>, Tatsuhiko Ozawa<sup>1,2</sup>, Kousei Ozawa<sup>3</sup>, Masayuki Shimojima<sup>4</sup>,  
4 Madoka Kawahara<sup>4</sup>, Fumi Kasuya<sup>5</sup>, Wakaba Okada<sup>5</sup>, Mami Nagashima<sup>5</sup>, Kenji  
5 Sadamasu<sup>5</sup>, Masae Itamochi<sup>6</sup>, Hideki Tani<sup>6</sup>, Yoshitomo Morinaga<sup>2,7</sup>, Kosuke Yuhara<sup>8</sup>,  
6 Jun Okamoto<sup>8</sup>, Haruna Ichikawa<sup>8</sup>, Takashi Kawahata<sup>8</sup>, Tomomi Yamazaki<sup>8</sup>, Masaharu  
7 Isobe<sup>1,2</sup>

8

9 <sup>1</sup> Department of Life Sciences and Bioengineering, Laboratory of Molecular and  
10 Cellular Biology, Faculty of Engineering, Academic Assembly, University of Toyama,  
11 3190 Gofuku, Toyama-shi, Toyama, 930-8555, Japan

12 <sup>2</sup> Center for Advanced Antibody Drug Development, University of Toyama, 3190  
13 Gofuku, Toyama-shi, Toyama, 930-8555, Japan

14 <sup>3</sup> Department of Life Sciences and Bioengineering, Laboratory of Molecular and  
15 Cellular Biology, Graduate School of Pharma-Medical Sciences, University of Toyama,  
16 3190 Gofuku, Toyama-shi, Toyama, 930-8555, Japan

17 <sup>4</sup> Department of Virology I, National Institute of Infectious Diseases, Toyama 1-23-1,  
18 Shinjuku-ku, Tokyo 162-8640, Japan

19 <sup>5</sup> Department of Microbiology, Tokyo Metropolitan Institute of Public Health, 3-24-1  
20 Hyakunincho, Shinjuku-ku, Tokyo, Japan

21 <sup>6</sup> Department of Virology, Toyama Institute of Health, 7-1 Nakataikoyama, Imizu-shi,  
22 Toyama 939-0363, Japan

23 <sup>7</sup> Department of Microbiology, Toyama University Graduate School of Medicine and  
24 Pharmaceutical Sciences, 2630 Sugitani, Toyama, 930-0194, Japan

25 <sup>8</sup> Biotechnology Research Laboratory, TOYOBO Co., Ltd., 10-24, Toyo-Cho,  
26 Tsuruga-Shi, Fukui, 914-8550, Japan

27

28 **Corresponding author**

29 Nobuyuki Kurosawa

30 [kurosawa@eng.u-toyama.ac.jp](mailto:kurosawa@eng.u-toyama.ac.jp)

31 Department of Life Sciences and Bioengineering, Laboratory of Molecular and Cellular  
32 Biology, Faculty of Engineering, Academic Assembly, University of Toyama, Toyama,  
33 Japan

34

## 35 **Abstract**

36 To address the global emergence of monkeypox after the 2022 epidemic, a rapid and  
37 accurate diagnostic tool is needed at the point of care to identify individuals infected with  
38 monkeypox virus (MPXV) to prevent and control the spread of the virus. We designed an  
39 antigen-detecting rapid diagnostic test that exclusively detects MPXV without  
40 cross-reacting with the vaccinia virus by developing monoclonal antibodies against the  
41 MPXV nuclear capsid protein A5L (MPXV-A5L). The test established a limit of  
42 detection sensitivity of 0.5 ng/mL of MPXV-A5L, with high sensitivity (87%) for  
43 clinical specimens collected from MPXV patients, a qPCR cycle threshold value  $\leq 25$   
44 and 100% specificity for qPCR-negative samples. The test is an ideal rapid diagnostic  
45 tool for supporting clinical decision-making for people suspected of having MPXV  
46 infection in resource-poor settings.

## 47 **Abbreviations**

48 antigen-detecting rapid diagnostic test, Ag-RDT; monkeypox virus, MPXV; orthopoxvirus,  
49 OPXV; quantitative polymerase chain reaction, qPCR; lateral flow  
50 immunochromatography assay, LFIA; vaccinia viruses, VACV; cycle threshold, Ct.

## 51 **Keywords**

52 Monkeypox; Antigen-detecting rapid diagnostic test; Monoclonal antibody; Lateral  
53 flow immunochromatography assay; qPCR; clinical evaluation

## 54 **1. Introduction**

55 Monkeypox is a zoonotic disease caused by the monkeypox virus (MPXV), a highly  
56 pathogenic double-stranded DNA virus classified in the genus orthopoxvirus (OPXV)

57 of the family *Poxviridae* (Karagoz et al., 2023; Mitja et al., 2023; Yu, Shi, and Cheng,  
58 2023). There are two genotypes of MPXV: Congo Basin strains (clade I) and West  
59 African strains (clades IIa and IIb). Although monkeypox was confirmed mainly in  
60 African countries, an epidemic of clade IIb MPXV was ongoing globally in early 2022,  
61 and 88,288 infected people and approximately 150 deaths were reported from 112  
62 countries on July 10, 2023 (Malik et al., 2023). Infection occurs through close contact  
63 with respiratory droplets, body fluids, skin lesions, or the blood of infected people or  
64 animals. After an incubation period ranging from 7 to 16 days, the affected individuals  
65 experience prodromal symptoms such as fever and general malaise, followed by the  
66 appearance of a skin rash that can be mistaken for those seen in chickenpox, measles,  
67 syphilis, and hand-foot-and-mouth disease (Zahmatyar et al., 2023) (Khattak et al.,  
68 2022) (Silva et al., 2023). Most healthy individuals experience mild disease progression,  
69 but immunocompromised patients, children, and pregnant women can experience severe  
70 symptoms (Schwartz et al., 2023; Silva et al., 2023). Older adults who have received  
71 smallpox vaccination acquired cross-protective immunity against MPXV. However,  
72 younger generations, who had not been vaccinated against smallpox, have no immunity  
73 to MPXV (Reynolds and Damon, 2012). Although the WHO declared the end of the  
74 monkeypox emergency, it called for sustained efforts for the long-term management of  
75 this virus (Bunge et al., 2022).

76 The detection of viral genes via polymerase chain reaction (PCR) is the gold standard  
77 method for MPXV diagnosis (Huang et al., 2023). However, these methods are  
78 designed for use in centralized laboratory settings. An antigen-detecting rapid  
79 diagnostic test (Ag-RDT) based on a lateral flow immunochromatography assay (LFIA)  
80 is an effective method for diagnosing MPXV through point-of-care testing in patients  
81 with monkeypox symptoms (Bunge et al., 2022). Several commercial and in-house  
82 Ag-RDTs have been developed for the diagnosis of MPXV by using antibodies against  
83 vaccinia virus (VACV) A27 or MPXV A29, an ortholog of VACV A29 (Mitja et al.,  
84 2023) (Huang et al., 2023; Hughes et al., 2014; Roumillat, Patton, and Davis, 1984).  
85 However, it is difficult to diagnose MPXV accurately, as most tests are not specific and  
86 may cross-react with VACV, which circulates in wild and domestic animals with  
87 occasional transmission to humans in close contact with these animals. Thus, an  
88 accurate MPXV Ag-RDT is vital for the effective treatment and control of MPXV  
89 infection, especially in areas where VACV is endemic (Miranda et al., 2017).

90 MPXV A5L, an ortholog of VACV A4L, is a highly conserved 39-kDa

91 immunodominant nucleocapsid protein that plays a role in the assembly and  
92 disassembly of the virion (Risco et al., 1999). The abundance and low mutation rate of  
93 MPXV A5L make it an ideal antigen for detecting MPXV via LFIA. In this work, we  
94 designed an MPXV Ag-RDT by developing a set of monoclonal antibodies that target  
95 MPXV A5L while not cross-reacting with VACV. We confirmed assay specificity via a  
96 panel of viral and bacterial pathogens. The MPXV Ag-RDT showed high sensitivity  
97 (87%) for clinical specimens collected from MPXV patients, with a qPCR cycle  
98 threshold (Ct) value  $\leq 25$  and a specificity of 100% for qPCR-negative samples. The  
99 MPXV Ag-RDT is suitable for point-of-care use in low-resource settings and can  
100 support the implementation of isolation measures to reduce the risk of transmission.

## 101 **2. Materials and methods**

### 102 **2.1 Ethics approval**

103 All animal and biosafety experiments were carried out at the University of Toyama and  
104 Toyama Institute of Health after approval from the Committee for Laboratory Animal  
105 Care and Use (A2022ENG-1 and G2022eng-1). Experiments with live VACV and  
106 MPXV were performed under biosafety levels 2 and 3, respectively, at the National  
107 Institute of Infectious Diseases. The clinical study was approved by the Ethical Review  
108 Board of the Tokyo Metropolitan Institute of Public Health (5 KenKenKen 3712).

### 109 **2.2 Antigen preparation**

110 Chemically synthesized MPXV A5L and VACA A4L cDNA were inserted into the  
111 pCold ProS2 vector (Takara Bio, Japan) and transformed into *E. coli* Tuner (DE3)  
112 pLacI (Novagen). Recombinant proteins were purified from the soluble fraction of the *E.*  
113 *coli* lysate via Ni-chelate affinity chromatography (Capturem His-tagged Purification  
114 Miniprep Kit, Takara Bio, Japan) followed by dialysis with PBS. The purified proteins  
115 were then concentrated using Amicon® Ultra-15 centrifugal filter units (EMD  
116 Millipore) and used as antigens. The MPXV peptide (LKDLMSSVEKDMRQLQAET)  
117 was conjugated to keyhole limpet hemocyanin (KLH) via the C-terminal cysteine  
118 residue.

### 119 **2.3 Immunization**

120 Anesthetized rats or rabbits were immunized three times intramuscularly at the tail base  
121 with 50 µg of A5L protein. Iliac lymph nodes were surgically removed from the  
122 euthanized animals. Anesthetized New Zealand White rabbits were immunized three  
123 times subcutaneously with 500 µg of KLH conjugates of MPXV A5L peptide, and  
124 peripheral blood lymphocytes were surgically corrected from the euthanized animals.

## 125 **2.4 Development of monoclonal antibodies**

126 The isolation of rat antigen-specific plasma cells was performed as previously described  
127 (Kurosawa et al., 2012). Briefly, rat lymph node cells fixed with ice-cold  
128 phosphate-buffered saline (PBS) containing 2% paraformaldehyde were stained with  
129 DyLight 488-labeled ProS-MPXV-A5L, DyLight 550-labeled ProS-Vaccinia-A4L,  
130 DyLight 650-labeled anti-rat IgG and DAPI in PBS containing 0.1% Triton X-100  
131 (PBST). MPXV A5L-specific plasma cells, defined as ProS-MPXV-A5L<sup>High</sup> and  
132 IgG<sup>High</sup>, were single-sorted via a JSAN Cell Sorter (Bay Bioscience). The isolation of  
133 rabbit antigen-specific plasma cells was performed as previously described (Ozawa et  
134 al., 2012). Briefly, IgG<sup>+</sup> cells isolated from A5L-immunized rabbits were cultured on a  
135 chip coated with 10 µg/mL rabbit IgG antibody at 37 °C for 3 hours. The chip was  
136 incubated with biotinylated MPXV A5L peptide (10 µg/mL) for 30 min and stained  
137 with Cy3-labeled streptavidin to detect antigen-specific plasma cells. Molecular cloning  
138 of immunoglobulin heavy and light chain genes from single-isolated plasma cells,  
139 followed by the expression of recombinant antibodies, was performed as previously  
140 described (Kurosawa et al., 2012; Ozawa et al., 2012). Antibodies were expressed via  
141 the Expi293 Expression System (Thermo Fisher Scientific) and purified using protein A  
142 affinity chromatography followed by size-exclusion chromatography (Cytiva).

## 143 **2.5 Immunofluorescence analysis**

144 A plasmid encoding Vaccinia A4L and a series of MPXV A5L mutants were  
145 constructed via PCR and inserted into the pCDNA3.1 or pEFMycHis plasmid. Each  
146 plasmid was transfected into HEK293 cells using the FuGENE 6 Transfection Reagent  
147 (Promega), and the cells were cultured for two days. After fixation with PBS containing  
148 4% paraformaldehyde, the cells were permeabilized with PBST and stained with the  
149 indicated antibodies. Images were captured with an Operetta High Content Imaging  
150 System (PerkinElmer) or a BZ-X700 all-in-one fluorescence microscope (Keyence).

## 151 **2.6 Preparation of a lateral flow immunochromatographic assay**

152 The #230-9 antibody (0.1 mg) and 100  $\mu$ L of NanoAct cellulose particles A (BL2: Dark  
153 Navy, Asahi Kasei Corporation) were mixed in 900  $\mu$ L of 10 mM Tris-HCl buffer (pH  
154 8.0) and allowed to stand at 37 °C for 120 minutes. The reaction was stopped by the  
155 addition of 12 mL of 100 mM boric acid buffer (pH 8.0) containing 1% casein. The  
156 antibody-cellulose particles suspended with 8 mL of 62 mM boric acid buffer (pH 9.2)  
157 containing 15% sucrose were uniformly applied to the entire surface of a glass fiber  
158 diagnostic pad (GFDX001050, Millipore) at an application rate of 60  $\mu$ L/cm, followed  
159 by drying at 45 °C for 30 minutes to prepare the conjugation pad. #2S-36 and  
160 goat-derived anti-rabbit IgG polyclonal antibodies were applied to Hi-Flow Plus 120  
161 Membrane Cards (HF120, Millipore) at predetermined locations in a volume of 1.0  
162  $\mu$ L/cm with a line width of approximately 1 mm. The membrane was dried for 30 min at  
163 40 °C. The conjugate pad was overlaid onto the nitrocellulose membrane with a 3 mm  
164 overlap. The sample pad and the absorbent pad were placed on either end of the  
165 nitrocellulose membrane with 3 mm and 5 mm of overlap, respectively. The  
166 immunochromatographic specimens were cut into strips 4 mm wide and 60 mm long  
167 and placed in a plastic cassette (K007, Shengfeng Plastic).

## 168 **2.7 Immunochromatographic device sensitivity evaluation**

169 Recombinant MPXV A5L was used as a quality control throughout the test  
170 manufacturing process. Recombinant MPXV A5L and virus-infected cell lysate were  
171 diluted with sample diluent solution (100 mM Tris buffer, pH 8.5, 0.877% sodium  
172 chloride, 0.2% Tween 20 and 0.9% Triton X), and an aliquot of 110  $\mu$ L was dispensed  
173 via pipette into the sample well of the cassette. After 15 minutes, the presence of lines  
174 was visually checked. Immediately after visual inspection, images were captured, and  
175 the signal intensity at both the test and control line locations was quantified using  
176 ImageJ (NIH).

## 177 **2.8 Viruses**

178 VACV and MPXV were propagated and titrated as described previously with a  
179 modification in that RK13 cells were used instead of Vero cells (Saijo et al., 2006). The  
180 SPL-2A7 strain (clade IIb) of MPXV was isolated using RK13 cells from specimens

181 derived from patients with suspected monkeypox and brought to the National Institute  
182 of Infectious Diseases for an administrative inspection of monkeypox.

## 183 **2.9 ELISA**

184 RK13 cells infected with VACV or MPXV were washed with PBS and treated with 1%  
185 NP40-containing PBS for cell lysis. Uninfected cells were also prepared and treated in  
186 parallel. The supernatants of the cell lysates were used as antigens for ELISA. ELISA  
187 plates (Nunc Maxisorp) were coated with cell lysates at a 1:1,000 dilution overnight,  
188 and blocking was performed with 5% skim milk. The plates were incubated with  
189 primary antibodies at the indicated concentrations, followed by further incubation with  
190 secondary antibodies labeled with horseradish peroxidase. Colorization was performed  
191 by the addition of ABTS (Roche), and the absorbance was measured at 405 nm with a  
192 microplate reader (Bio-Rad iMark).

## 193 **2.10 Clinical sample collection and real-time qPCR assay**

194 The samples sent to the Tokyo Metropolitan Institute of Public Health (TMIPH) as a  
195 part of the active epidemiological surveillance of suspected cases of monkeypox were  
196 used for this study. Viral DNA was extracted from the samples (skin lesions: crusts and  
197 blister swabs) via a QIAamp DNA Mini Kit (Qiagen, Hilden, Germany). Real-time  
198 qPCR to detect MPXV (targeting the F3L region) was performed using a QuantStudio  
199 12K Flex (Thermo Fisher Scientific, Waltham, MA, USA) and a QuantiTect Probe PCR  
200 Kit (Qiagen) according to the pathogen detection manual of the National Institute of  
201 Infectious Diseases, Japan  
202 (<https://www.niid.go.jp/niid/images/lab-manual/mpox20230531.pdf>). The viral load of  
203 the MPXV was expressed as the Ct value detected by real-time PCR as previously  
204 described (Kasuya et al., 2023).

## 205 **2.11 Statistical analysis**

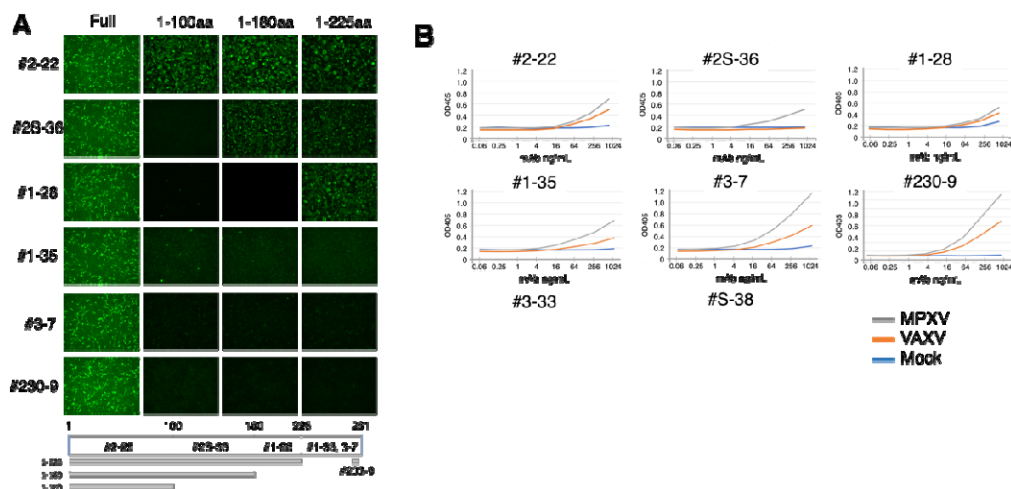
206 The sensitivity, specificity, positive predictive value, and negative predictive value were  
207 estimated via the Clopper-Pearson exact method, along with corresponding 95%  
208 confidence intervals.

209

## 210 3. Results

### 211 3.1 Development and screening of mAbs against A5L

212 To develop anti-MPXV A5L antibodies, we immunized rats with recombinant MPXV  
 213 A5L and rabbits with the KLH-conjugated MPXV A5L peptide. Immunoglobulin heavy  
 214 and light chain gene cloning from antigen-specific single plasma cells resulted in the  
 215 production of 128 rat and three rabbit mAbs. The activity of these mAbs was examined  
 216 via immunofluorescence staining of HEK293 cells expressing MPXV A5L. Among the  
 217 61 MPXV A5L-positive mAbs tested, five rat mAb clones and one rabbit mAb clone  
 218 were selected on the basis of their unique complementarity-determining region 3  
 219 sequences. Epitope mapping of these mAbs by using HEK293 cells expressing a series  
 220 of N-terminal deletion mutants of MPXV A5L revealed that the epitope for #2-22 was  
 221 located on amino acids 1-100, #2S-36 on amino acids 100-180, #1-28 on amino acids  
 222 180-225 and #1-35, #3-7, and #230-9 on amino acids 225-281 (Fig. 1). For further  
 223 characterization of these mAbs, an ELISA screen was performed using MPXV- or  
 224 VACV-infected Vero cell lysates as antigens (Fig. 1B). #1-28, #1-35, #2-22, #3-7, and  
 225 #230-9 reacted with the MPXV- and VACV-infected cell lysates. #2S-36 reacted with  
 226 only the MPXV-infected cell lysate.



227

228

229 Fig. 1. Antibody development for MPXV detection.



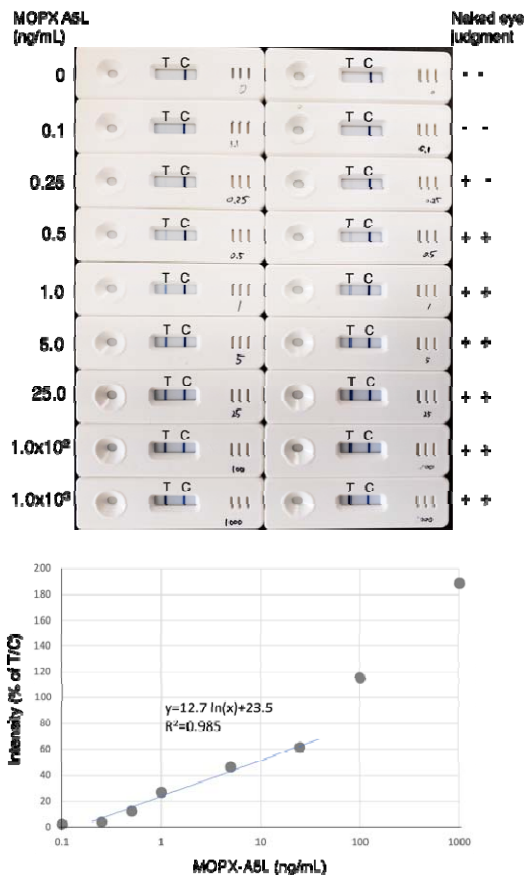
230 (A) Immunofluorescence images of HEK293 cells expressing a series of C-terminal  
231 deletion mutants of MPXV A5L stained with the indicated mAbs. A schematic diagram  
232 of the deletion mutants of MPXV A5L; the locations of the epitopes for each mAb are  
233 shown.

234 (B) ELISA screening of mAbs using MPXV (SPL-2A7, a clade IIb strain isolated in  
235 2022 in Japan), VACV (strain LC16m8), or mock-infected RK13 cell lysates as the  
236 antigen. The cells were lysed in 1% NP40/PBS, and the supernatants, which were  
237 diluted 1000-fold in PBS, were added to each well of a 96-well plate. Serially diluted  
238 mAbs were added to the plates. The figure reports the values from a single experiment.

239 These results indicate that #2S-36 is a suitable antibody that can differentiate MPXV  
240 from VACV. An ELISA was performed to select clones to be paired with #2S-36. The  
241 results revealed that #1-28, #3-7, #1-35, and #230-9 had nearly identical sensitivities for  
242 MPXV A5L, whereas 2-22 did not (Supplemental Fig. 1A). Among these clones,  
243 #230-9, which recognizes the C-terminus of MPXV A5L and partially cross-reacted  
244 with VACV, was selected.

### 245 **3.2 Development of a rapid antigen test for the detection of MPXV**

246 The #2S-36/#230-9 set was tested in immunochromatography pairs, with one antibody  
247 conjugated to cellulose nanoparticles and one antibody absorbed into a nitrocellulose  
248 membrane. The test strips prepared by colloidal cellulose labeling with #230-9 and  
249 T $\square$  lines with #2S-36 presented greater detection sensitivity than the reverse  
250 combination did (Supplemental Fig. 1B). The kinetic analyses by surface plasmon  
251 resonance highlighted the fast association ( $k_{on}$ ) and slow dissociation ( $k_{off}$ ) rates for  
252 the interaction with MPXV A5L, resulting in equilibrium dissociation constants ( $K_D$   
253 values) of  $0.82 \times 10^{-9}$  M for #230-9 and  $1.5 \times 10^{-9}$  M for #2S-36, respectively  
254 (Supplemental Fig. 2). Based on the test strips assay, an Ag-RDT was established with  
255 #2S-36 used as a capture Ab in the test (T) line and colloidal cellulose labeled #230-9 as  
256 a detection Ab absorbed on a pad. The control (C) line was incubated with a goat  
257 anti-rabbit IgG antibody. The analytical performance of the Ag-RDT was evaluated by  
258 testing the recombinant MPXV A5L as a standard sample in the concentration range of  
259 0 to -1000 ng/mL. Naked-eye observation revealed that the A5L concentration of 0.5  
260 ng/mL caused a slight but distinguishable difference in the test line intensity compared  
261 with that of the negative control (Fig. 2).



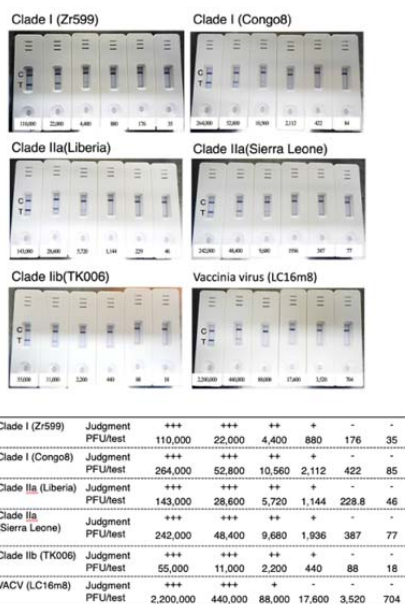
262

263 Fig. 2 Limit of detection of the MPXV Ag-RDT using recombinant MPXV A5L as the  
264 antigen.

265 (A) Photographs representing the LFIA strips and test zones. Recombinant MPXV A5L  
266 diluted with sample diluent solution and an aliquot of 110  $\mu$ L was dropped into the  
267 immunochromatographic device. After 15 minutes, the presence of lines was visually  
268 checked. Immediately after visual inspection, images were captured, and the signal  
269 intensity at both the test and control line locations was quantified via ImageJ. The  
270 results of two experimental replicates are shown. The visual limit of detection was set  
271 by two independent observers at the lowest A5L concentration at which the T line  
272 disappeared in the two strips. Naked-eye judgment: positive (+) or negative (-). C,  
273 control. T, test.

274 (B) Standard curve plot of the T/C value (%) on the Y-axis and the logarithm of MPXV  
275 A5L on the X-axis.

276 A standard curve was generated by plotting the relative band intensity ratio (T/C)  
 277 against the MPXV A5L concentration, which increased with increasing protein  
 278 concentration. It was quantitative in the range of 0 to 25.0 ng/mL, with a correlation  
 279 coefficient of 0.9994. Increasing the antigen concentration above 1000 ng/mL led to a  
 280 decrease in the intensity of the C line, whereas the intensity of the T line continued to  
 281 increase, affecting the T/C ratio. This is likely due to fewer free-capture antibodies  
 282 binding to the C line, as more antibodies are used to form immune complexes. The limit  
 283 of detection (LOD) of the Ag-RDT was 440 plaque-forming units (PFU)/test for clade  
 284 I Ib SPL-2A7 and 2112 PFU/test for clade I Congo8 virus. Cross-reactivity with VACV  
 285 was not detected at concentrations under  $1.76 \times 10^4$  PFU/test (Fig. 3). The Ag-RDT did  
 286 not cross-react with viruses causing diseases with symptoms similar to those of MPXV,  
 287 such as the measles virus, Coxsackie virus type A6, A16, and enterovirus A71  
 288 (Supplemental Fig. 3). The Ag-RDT was negative for all 20 bacterial lysates present in  
 289 the airway and oral cavity (Supplemental Fig. 4).



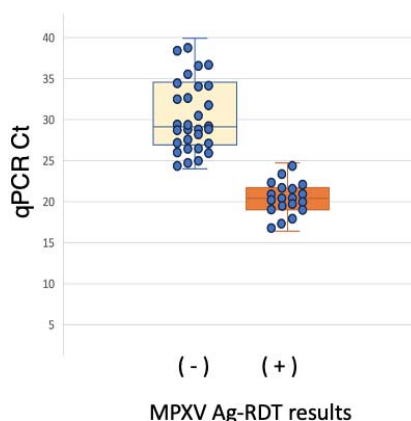
290

291 Fig. 3 Analytical sensitivity and specificity of the MPXV Ag-RDT using serially diluted  
 292 stocks of isolates of MPXV or VACV. An aliquot of 75  $\mu$ l of the viral mixture was  
 293 diluted with 75  $\mu$ l of sample dilution buffer, and 110  $\mu$ l was subsequently added to the  
 294 cassette. Visual judgment was independently determined by two people.

295 When concentrations of human or bovine serum, ranging from 0.2% to 8%, were spiked  
296 with MPXV (11,000 PFU) and then applied to the Ag-RDT, no significant inhibition of  
297 the test line intensity was observed, indicating that the serum did not significantly affect  
298 the performance of the assay (Supplemental Fig. 5).

### 299 3.3 Point-of-care clinical evaluation studies

300 We next conducted a study to compare the sensitivity of the Ag-RDT with that of qPCR  
301 for MPXV clinical specimens collected as dry swabs (Kasuya et al., 2023). The  
302 qPCR-positive samples were divided into high (Ct value of  $\leq 25$ ) and low (Ct value of  
303 26~40) groups. As shown in Fig. 4 and Table 1, The Ag-RDT detected 87% (20 out of  
304 23 swabs; 95% CI, 66%-97%) of the samples in the high group but failed to detect  
305 samples in the low group (0 out of 27 swabs; 95% CI, 0%-13%). The Ag-RDT results  
306 were consistent with those of the qPCR-negative samples, with a specificity of 100% (0  
307 out of 10 swabs; 95% CI, 0%-31%).



308

309 Fig. 4. The MPXV Ag-RDT-positive and antigen-negative samples were compared via  
310 a box plot of the qPCR Ct values. Each symbol represents one sample. The center lines  
311 show the medians. The box limits are quartiles 1 and 3, and the whiskers represent the  
312 maximum and minimum values.

### 313 4. Discussion

314 In this study, we designed an MPXV Ag-RDT by developing an antibody set that can  
315 differentiate MPXV from VACV. The Ag-RDT provided accurate results in less than 15

316 minutes and exhibited high selectivity and analytical sensitivity for MPXV. A  
317 concordance study of clinical specimens collected as dry swabs revealed that the  
318 Ag-RDT showed 87% sensitivity in samples with Ct values of  $\leq 25$  and a specificity of  
319 100% with qPCR-negative samples.

320 Since the global outbreak of monkeypox in 2022, combined with the increasing danger  
321 of other zoonotic orthopoxvirus infections, there has been a need to develop a  
322 MPXV-specific diagnostic tests. Among the MPXV proteins, the virus envelope protein  
323 A29, which plays an important role in virus-host cell interactions, is one of the most  
324 extensively studied targets (Ahsendorf et al., 2019; Bengali, Satheshkumar, and Moss,  
325 2012; Howard, Senkevich, and Moss, 2008). Several in-house and commercial  
326 Ag-RDTs have been developed by using antibodies specific to A29. However, most of  
327 these are cross-reactive with VACV (de Lima et al., 2023; Dubois, Hammarlund, and  
328 Slifka, 2012). Owing to the increasing incidence of occasional outbreaks of VACV in  
329 South America, the use of such tests can result in misdiagnosis as MPXV (Miranda et  
330 al., 2017). Recently, mAbs that can distinguish MPXV from VACV have been  
331 developed and applied to Ag-RDTs (Davis et al., 2023; Hughes et al., 2014; Ye et al.,  
332 2023). Although MPVX typically displays a low number of mutations, such as those  
333 associated with DNA viruses, the mutation ratio of MPVX isolated after the 2022  
334 outbreak surpassed the standard mutation rate of the virus (Yashavardhan et al., 2023).  
335 Consequently, antibodies that recognize the A29 epitope may not work as effectively in  
336 the future because of viral mutations, which could cause decreased sensitivity and  
337 inaccurate results. To prepare for unexpected mutant strains of MPXV that may evade  
338 current tests, it is crucial to develop an additional set of antibodies targeting a different  
339 protein of MPXV.

340 Among orthopoxviruses, MPXV A5L is one of the major core immunogenic and  
341 conserved proteins (Risco et al., 1999). The two antibodies targeting MPXV A5L are  
342 suitable for use in rapid diagnostic tests because they can bind to a distant epitope with  
343 a high association rate constant ( $k_{on}$ ) and a low dissociation rate constant ( $k_{off}$ ). These  
344 characteristics enable the antibodies to quickly bind to the antigen and maintain strong  
345 binding. This makes them ideal for designing species-specific serological assays  
346 targeting MPXV A5L. No cross-reactivity was observed for viruses causing diseases  
347 with symptoms similar to those of monkeypox, bacteria present in the airway and oral  
348 cavity and interfering substances in the serum. No loss of sensitivity was observed in

349 this test when the samples were stored at room temperature for one year after  
350 manufacturing.

351 The viral load has been found to be the most important factor for determining antigen  
352 test sensitivity (Lim et al., 2023). Our data showed that the Ag-RDT has enough  
353 sensitivity to identify contagious patients with  $Ct \leq 25$ . Therefore, this test could guide  
354 initial decisions regarding isolation and management and reduce the need for a qPCR  
355 test in the case of positive results. It is important to note that the sensitivity of the test  
356 decreased when the qPCR Ct value was greater than 25. As a result, this test may not be  
357 appropriate for detecting the virus in the prodromal stage, as the viral load may be too low to  
358 be detected by the Ag-RDT. Prior to clinical implementation, this device requires several  
359 improvements to enhance its sensitivity and performance.

## 360 **Conclusion**

361 The MPXV Ag-RDT is capable of sensitive and specific detection of MPXV in  
362 virus-infected clinical specimens, distinguishing it from other skin infections. The  
363 MPXV Ag-RDT has potential for use in point-of-care settings.

## 364 **Transparency declaration**

365 All the authors have nothing to disclose.

## 366 **Funding**

367 This research was supported by grants from the Japan Agency for Medical Research and  
368 Development (AMED) to Masaharu Isobe (19187977, 20333128 and 22723616) and  
369 Tatsuhiko Ozawa (JP24ama121010), as well as from The Toyama Pharmaceutical  
370 Valley Development Consortium (no grant number assigned) to Masaharu Isobe and  
371 Japan Society for the Promotion of Science, Japan (Grant in Aid for Scientific Research  
372 B) (22H02875) to Nobuyuki Kurosawa. The funders had no role in the study design,  
373 data collection and analysis, publishing decisions, or the preparation of the manuscript.

## 374 **CRedit authorship contribution statement**

375 Nobuyuki Kurosawa: Writing – original draft, Methodology, Investigation, Formal  
376 analysis, Data curation. Tatsuhiko Ozawa: Methodology, Investigation, Formal analysis.

377 Madoka Kawahara: Methodology, Investigation, Formal analysis. Masayuki  
378 Shimojima: Methodology, Investigation, Formal analysis. Madoka Kawahara:  
379 Methodology, Investigation, Formal analysis. Fumi Kasuya: Methodology,  
380 Investigation, Formal analysis. Wakaba Okada: Methodology, Investigation, Formal  
381 analysis. Mami Nagashima: Methodology, Investigation, Formal analysis. Kenji  
382 Sadamasu: Methodology, Investigation, Formal analysis. Masae Itamochi: Methodology,  
383 Investigation, Formal analysis. Hideki Tani: Methodology, Investigation, Formal  
384 analysis. Yoshitomo Morinaga: Methodology, Investigation, Formal analysis. Masaharu  
385 Isobe: Funding acquisition, Supervision.

### 386 **Declaration of competing interest**

387 The authors declare that they have no known competing financial interests or personal  
388 relationships that could have appeared to influence the work reported in this paper.

### 389 **Data availability**

390 The data will be made available upon request.

### 391 **Acknowledgments**

392 We thank past and current members of our laboratory for fruitful discussions. We also  
393 thank Y. Nohara and K Takai for their technical support.

### 394 **References**

395 Ahsendorf, H.P., Gan, L.L., Eltom, K.H., Abd El Wahed, A., Hotop, S.K., Roper, R.L.,  
396 Beutling, U., Broenstrup, M., Stahl-Hennig, C., Hoelzle, L.E. and Czerny, C.P.,  
397 2019. Species-Specific Conservation of Linear Antigenic Sites on Vaccinia  
398 Virus A27 Protein Homologs of Orthopoxviruses. *Viruses* 11.  
399 Bengali, Z., Satheshkumar, P.S. and Moss, B., 2012. Orthopoxvirus species and strain  
400 differences in cell entry. *Virology* 433, 506-12.  
401 Bunge, E.M., Hoet, B., Chen, L., Lienert, F., Weidenthaler, H., Baer, L.R. and Steffen,  
402 R., 2022. The changing epidemiology of human monkeypox-A potential threat?  
403 A systematic review. *PLoS Negl Trop Dis* 16, e0010141.  
404 Davis, I., Payne, J.M., Olguin, V.L., Sanders, M.P., Clements, T., Stefan, C.P.,  
405 Williams, J.A., Hooper, J.W., Huggins, J.W., Mucker, E.M. and Ricks, K.M.,

- 406           2023. Development of a specific MPXV antigen detection immunodiagnostic  
407           assay. *Front Microbiol* 14, 1243523.
- 408   de Lima, L.F., Barbosa, P.P., Simeoni, C.L., de Paula, R.F.O., Proenca-Modena, J.L.  
409           and de Araujo, W.R., 2023. Electrochemical Paper-Based Nanobiosensor for  
410           Rapid and Sensitive Detection of Monkeypox Virus. *ACS Appl Mater Interfaces*  
411           15, 58079-58091.
- 412   Dubois, M.E., Hammarlund, E. and Slifka, M.K., 2012. Optimization of peptide-based  
413           ELISA for serological diagnostics: a retrospective study of human monkeypox  
414           infection. *Vector Borne Zoonotic Dis* 12, 400-9.
- 415   Howard, A.R., Senkevich, T.G. and Moss, B., 2008. Vaccinia virus A26 and A27  
416           proteins form a stable complex tethered to mature virions by association with the  
417           A17 transmembrane protein. *J Virol* 82, 12384-91.
- 418   Huang, X., Xiao, F., Jia, N., Sun, C., Fu, J., Xu, Z., Cui, X., Huang, H., Qu, D., Zhou, J.  
419           and Wang, Y., 2023. Loop-mediated isothermal amplification combined with  
420           lateral flow biosensor for rapid and sensitive detection of monkeypox virus.  
421           *Front Public Health* 11, 1132896.
- 422   Hughes, L.J., Goldstein, J., Pohl, J., Hooper, J.W., Lee Pitts, R., Townsend, M.B.,  
423           Bagarozzi, D., Damon, I.K. and Karem, K.L., 2014. A highly specific  
424           monoclonal antibody against monkeypox virus detects the heparin binding  
425           domain of A27. *Virology* 464-465, 264-273.
- 426   Karagoz, A., Tombuloglu, H., Alsaed, M., Tombuloglu, G., AlRubaish, A.A.,  
427           Mahmoud, A., Smajlovic, S., Cordic, S., Rabaan, A.A. and Alsuhaime, E., 2023.  
428           Monkeypox (mpox) virus: Classification, origin, transmission, genome  
429           organization, antiviral drugs, and molecular diagnosis. *J Infect Public Health* 16,  
430           531-541.
- 431   Kasuya, F., Negishi, A., Kumagai, R., Yoshida, I., Murakami, K., Fujiwara, T.,  
432           Hasegawa, M., Harada, S., Amano, A., Inada, M., Saito, S., Morioka, S.,  
433           Ohmagari, N., Sugishita, Y., Miyake, H., Nagashima, M., Sadamasu, K. and  
434           Yoshimura, K., 2023. Genetic Characteristics of the Virus Detected in the First  
435           Mpox Imported Case in Tokyo, Japan. *Jpn J Infect Dis* 76, 259-262.
- 436   Khattak, S., Rauf, M.A., Ali, Y., Yousaf, M.T., Liu, Z., Wu, D.D. and Ji, X.Y., 2022.  
437           The monkeypox diagnosis, treatments and prevention: A review. *Front Cell*  
438           *Infect Microbiol* 12, 1088471.
- 439   Kurosawa, N., Yoshioka, M., Fujimoto, R., Yamagishi, F. and Isobe, M., 2012. Rapid  
440           production of antigen-specific monoclonal antibodies from a variety of animals.  
441           *BMC Biol* 10, 80.



- 442 Lim, C.K., McKenzie, C., Deerrain, J., Chow, E.P.F., Towns, J., Chen, M.Y., Fairley,  
443 C.K., Tran, T. and Williamson, D.A., 2023. Correlation between monkeypox  
444 viral load and infectious virus in clinical specimens. *J Clin Virol* 161, 105421.
- 445 Malik, S., Ahmed, A., Ahsan, O., Muhammad, K. and Waheed, Y., 2023. Monkeypox  
446 Virus: A Comprehensive Overview of Viral Pathology, Immune Response, and  
447 Antiviral Strategies. *Vaccines (Basel)* 11.
- 448 Miranda, J.B., Borges, I.A., Campos, S.P.S., Vieira, F.N., de Azara, T.M.F., Marques,  
449 F.A., Costa, G.B., Luis, A., de Oliveira, J.S., Ferreira, P.C.P., Bonjardim, C.A.,  
450 da Silva, S.L.M., Eiras, A.E., Abrahao, J.S., Kroon, E.G., Drumond, B.P., Paglia,  
451 A.P. and Trindade, G.S., 2017. Serologic and Molecular Evidence of Vaccinia  
452 Virus Circulation among Small Mammals from Different Biomes, Brazil. *Emerg*  
453 *Infect Dis* 23, 931-938.
- 454 Mitja, O., Ogoina, D., Titanji, B.K., Galvan, C., Muyembe, J.J., Marks, M. and Orkin,  
455 C.M., 2023. Monkeypox. *Lancet* 401, 60-74.
- 456 Ozawa, T., Piao, X., Kobayashi, E., Zhou, Y., Sakurai, H., Andoh, T., Jin, A., Kishi, H.  
457 and Muraguchi, A., 2012. A novel rabbit immunospot array assay on a chip  
458 allows for the rapid generation of rabbit monoclonal antibodies with high  
459 affinity. *PLoS One* 7, e52383.
- 460 Reynolds, M.G. and Damon, I.K., 2012. Outbreaks of human monkeypox after  
461 cessation of smallpox vaccination. *Trends Microbiol* 20, 80-7.
- 462 Risco, C., Rodriguez, J.R., Demkowicz, W., Heljasvaara, R., Carrascosa, J.L., Esteban,  
463 M. and Rodriguez, D., 1999. The vaccinia virus 39-kDa protein forms a stable  
464 complex with the p4a/4a major core protein early in morphogenesis. *Virology*  
465 265, 375-86.
- 466 Roumillat, L.F., Patton, J.L. and Davis, M.L., 1984. Monoclonal antibodies to a  
467 monkeypox virus polypeptide determinant. *J Virol* 52, 290-2.
- 468 Saijo, M., Ami, Y., Suzaki, Y., Nagata, N., Iwata, N., Hasegawa, H., Ogata, M.,  
469 Fukushi, S., Mizutani, T., Sata, T., Kurata, T., Kurane, I. and Morikawa, S.,  
470 2006. LC16m8, a highly attenuated vaccinia virus vaccine lacking expression of  
471 the membrane protein B5R, protects monkeys from monkeypox. *J Virol* 80,  
472 5179-88.
- 473 Schwartz, D.A., Ha, S., Dashraath, P., Baud, D., Pittman, P.R. and Waldorf, K.A., 2023.  
474 Mpox Virus in Pregnancy, the Placenta, and Newborn. *Arch Pathol Lab Med*  
475 147, 746-757.
- 476 Silva, M.S., Coutinho, C., Torres, T.S., Peixoto, E.M., Bastos, M.O., Mesquita, M.B.,  
477 Tavares, I.C., Andrade, H.B., Reges, P.P., Martins, P.S., Echeverria-Guevara, A.,

478           Moreira, R.I., Lessa, F.C.S., Hoagland, B., Nunes, E.P., Cardoso, S.W., Veloso,  
479           V.G., Grinsztejn, B. and Group, I.N.-F.M.S., 2023. Mpox severity and  
480           associated hospitalizations among people living with HIV and related  
481           immunosuppression in Brazil. *AIDS*.

482           Yashavardhan, M.H., Bohra, D., Rana, R., Tuli, H.S., Ranjan, V., Rana, D.S. and  
483           Ganguly, N.K., 2023. Comprehensive overview of 2022 human monkeypox  
484           outbreak and its pathology, prevention, and treatment: A strategy for disease  
485           control. *Microbiol Res* 277, 127504.

486           Ye, L., Lei, X., Xu, X., Xu, L., Kuang, H. and Xu, C., 2023. Gold-based paper for  
487           antigen detection of monkeypox virus. *Analyst* 148, 985-994.

488           Yu, X., Shi, H. and Cheng, G., 2023. Mpox Virus: Its Molecular Evolution and  
489           Potential Impact on Viral Epidemiology. *Viruses* 15.

490           Zahmatyar, M., Fazlollahi, A., Motamedi, A., Zolfi, M., Seyedi, F., Nejadghaderi, S.A.,  
491           Sullman, M.J.M., Mohammadinasab, R., Kolahi, A.A., Arshi, S. and Safiri, S.,  
492           2023. Human monkeypox: history, presentations, transmission, epidemiology,  
493           diagnosis, treatment, and prevention. *Front Med (Lausanne)* 10, 1157670.

494